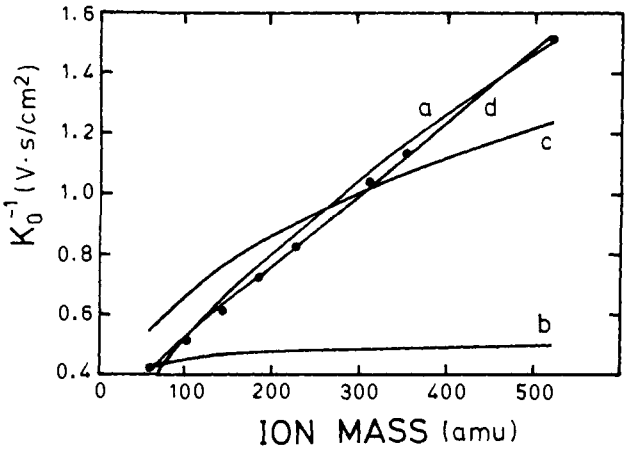

Figure 6. The measured inverse mobility, at 200 °C in air, of a homologous series of protonated normal tertiary aliphatic amines as a function of ion mass. Curve a was calculated according to the rigid sphere model (r_0 = 4.1 Å); curve b according to the polarization limit model; curve c according to the hard-core model with a^* = 0.1, z = 0 Å/amu, and r_0 = 3.31 Å; and curve d with a^* = 0.1, z = 0.0025 Å/amu, and r_0 = 2.53 Å.

Tables I–III). These calculated values depend on a^*, as evident from eq 5. In air, the curve-fitting procedure is strongly dependent on the choice of a^*, with a^* = 0.2 giving the best fit. The quality of the fit diminishes by changing a^*. In the acetyls (Figure 1), aromatic amines (Figure 2), and all aliphatic amines (Figure 4), taking a^* = 0.2 gave the best fit (as expressed by X^2), while in the normal tertiary amines (Figure 6) a somewhat better fit was obtained with a^* = 0.1. In helium, variation of a^* from 0 to 0.3 barely affected the quality of the fit, while taking a^* = 0.4 had only a small effect (Figure 3).

As mentioned above, the values of r_m and Ω_D, and especially of ϵ_0, depend strongly on the choice of a^*. Therefore, as the purely mathematicaly fitting procedure is insensitive to variation of a^*, it must be selected from physical considerations. There is no experimental data from other techniques, except IMS, on the strength of the ion–helium interaction. The fact that the attractive interaction of a given ion with helium is weaker than in air is an indication on the choice of a^*. Thus, taking a large value (a^* = 0.4) for helium would yield an unreasonably large calculated interaction potential; therefore, a^* = 0.1 was chosen for helium.

In conclusion, it appears that taking a^* = 0.2 for ions in air and a^* = 0.1 in helium is an a priori reasonable choice for these ions in all cases. It is especially interesting to compare the collision cross sections. First, the values obtained are in good agreement with those reported by Hagen.[17] Second, evidently the collision cross section for a given ion in helium is about half that in air.

Finally, one can use the rigid sphere approximation to calculate the radius of the ion (from the sum of radii). For protonated pyridine, for example, the result would be about 3.8 Å, which reasonably agrees with the ab initio calculations of Del-Bene.[18] Thus, although this approximation poorly reproduces mobility results, it can give a crude estimate of the ion radius once the collision cross section has been derived from the mobility measurements. Comparison of the results obtained for Ω_D, r_m, and ϵ_0 for ions drifting through helium and through air gives an insight as to the differences in the ion–neutral interactions. For a given ion, the collision cross section is about double the size in air than in helium, which reflects the relative size of the neutral species. The depth of the minimum (ϵ_0) in the interaction potential is smaller in helium by an order of magnitude, while r_m differs by less than 25%. The difference in size between helium atoms and the air (nitrogen and oxygen) molecules, which causes the collision cross-section differences, also partly accounts for the somewhat smaller r_m in helium. On the other hand, the difference between the polarizability of helium and of air leads to a much weaker attractive interaction between the ion and helium atoms. Thus, the difference in size leads to a smaller collision cross section in helium, and the polarizability difference leads to a stronger interaction of the ion with air, resulting in mobilities in helium that are higher by a factor of 3–5 than in air.

The introduction of the correction factor, z, enhanced the agreement between the measured data points and the calculations based on the hard-core model. This improvement was evident especially for the mobility measurements of polyatomic ions in helium and for mobility measurements of ions with masses above 200 amu, in air. As most of the earlier studies were concerned with a limited mass range of ions, and with air or nitrogen as drift gases, the problem of a quantitative fit was not as severe and did not arise.

Registry No. He, 7440-59-7.

(17) Hagen, D. F. In *Plasma Chromatography*; Carr, T. W., Ed.; Plenum Press: New York, 1984; Chapter 4.
(18) Del-Bene, J. E. *J. Am. Chem. Soc.* **1975**, *97*, 5330.

Direct Measurement of the Enthalpy Difference between Enol and Keto Forms by the Time-Resolved Thermal Lens Method: 7-Hydroxyquinoline

Masahide Terazima* and Tohru Azumi

Contribution from the Department of Chemistry, Faculty of Science, Tohoku University, Sendai, 980, Japan. *Received September 6, 1988*

Abstract: The enthalpy difference between the keto and enol forms of 7-hydroxyquinoline is measured by using the time-resolved thermal lens technique. The obtained large difference, 3400 cm^{-1}, in the ground state and −4200 cm^{-1} in the excited singlet state indicate the predominant enol form in the ground state and keto form in the excited state.

1. Introduction

A protropic tautomerism of heteroaromatic compounds containing a hydroxy group at the excited state has long been of interest to chemists and has attracted further attention in recent years. For such molecules, electronic excited states of keto and enol forms have been investigated extensively by using absorption and/or emission spectroscopy.[1-7] Although the enthalpy difference (ΔH) between the keto and enol forms is one of the important

(1) Huppert, D.; Gutman, M.; Kaufmann, K. J. In *Photoselective Chemistry*; Jortner, J., Levine, R. D., Rice, S. A., Eds.; Wiley: New York, 1981; Vol. 2.

0002-7863/89/1511-3824$01.50/0

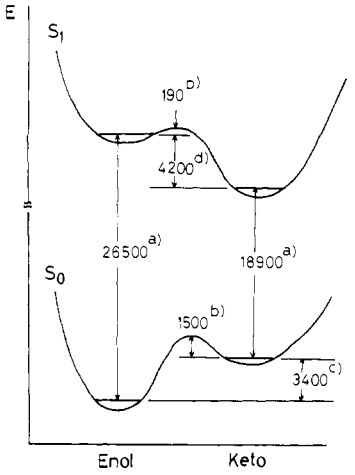

Figure 1. Schematic energy diagram of the proton transfer in 7-hydroxquinoline (in cm^{-1}). The experimental results obtained in this paper and the reported parameters are used. (a) Transition energies taken from ref 4 and 5; (b) activation energies taken from ref 4; (c) those obtained from the present experimental results; (d) those obtained from $E_f^e - E_f^k - \Delta H$.

quantities to elucidate the kinetics of such a proton-transfer system, few data are available.[2] If ΔH is small compared with the thermal energy, it can be determined from the temperature dependence of the equilibrium constant.[2] Unfortunately, however, ΔH is much larger than thermal energy in many proton-transfer systems, and in this case, the equilibrium constant becomes small and the measured ΔH by the temperature-dependence method is less reliable. In this paper, we demonstrate that the time-resolved thermal lens (TL) technique is a very powerful method to determine ΔH even in the case of a large ΔH. As a typical example, we applied this method to 7-hydroxyquinoline in methanol.

When a ground-state solute molecule in solvent is excited to higher electronic states by irradiation, the temperature and hence the refractive index of the solvent change due to the heat released by the radiationless transition from the excited solute molecule. In the TL method, the refractive index profile is probed optically as a divergent lens.[8] Therefore, this method has a great advantage to detect a weak or nonemissive transition, such as singlet–triplet transition or enol–keto transformation. Recently, we applied the time-resolved TL method to measure the quantum yield of triplet formation in liquid phase[9] and in solid phase.[10] As a extension of the application, in this paper, we report that the heat coming from the process of keto–enol tautomerism can be determined by this method.

2. Experimental Section

2.1. Method. The enol form of 7-hydroxyquinoline is known to be much more stable than the keto form, and only the enol form exists in a room temperature solution.[3-7,11] In the excited state, the nitrogen is more basic and the phenolic group more acidic as compared with the ground state. Then in the lowest excited singlet (S_1) state, the keto form is created by proton transfer from the enol form and the S_1 state of the keto form decays to the ground state of the keto form.[3-6] The keto form of the ground state then transfers to the enol form by proton back-transfer (Figure 1). During these processes, the slow process is only the proton back-transfer process in the ground state and the rate of the other processes are faster than the time resolution of the TL method (the order of submicroseconds).[4,5] Therefore, the thermal lens signal that is created by the nonradiative decay should first rise within submicroseconds and should then rise slowly corresponding to the rate of the proton back-transfer. The ratio of the total signal intensity (U_t) to the slow-rise signal intensity (U_s) is expressed by

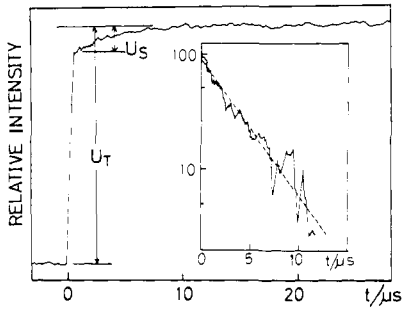

Figure 2. Time dependence of the thermal lens signal after the excitation of 7-hydroxquinoline in methanol. Inset: semilog plot of the rise curve.

$$\frac{U_s}{U_t} = \frac{\Delta H \phi_t}{E_{ex} - E_f^e \phi_f^e - E_f^k \phi_f^k} \quad (1)$$

where ϕ_t is the quantum yield of the proton transfer at the S_1 state. E_{ex}, E_f^e, and E_f^k are the photon energy that is used to excite the molecule and the energy of the fluorescent state of the enol and that of the keto forms, respectively. ϕ_f^e and ϕ_f^k are the quantum yields of the fluorescence of the enol and keto forms, respectively.

2.2. Apparatus. The experimental setup for the time-resolved TL method was reported previously.[9,10] Briefly, a nitrogen laser (Molectron UV-24) and a He–Ne laser were used for the excitation and monitoring laser. The N_2 laser beam was focused inside the square sample cell with a 20-cm focal lens. The He–Ne laser beam, which was made collinear with the N_2 laser beam, was detected by a photomultiplier tube (Hamamatsu R-928) through a pin hole. The obtained signal was averaged by a transient digitizer (Iwatsu DM-901) and a microcomputer.

7-Hydroxyquinoline, purchased from Eastman Kodak Co., was purified by recrystallization. The solvent, methanol, was purified by distillation.

3. Results and Discussion

The time dependence of the TL signal of 7-hydroxyquinoline in methanol is shown in Figure 2. The TL signal decays with a time constant of thermal diffusion (order of milliseconds). At the initial part of the signal, a fast rising of nanosecond order and a slow rising of microsecond order components is observed. The time constant of the fast-rising component is determined by the time constant of the thermal lens signal, namely w/v, where w is the beam radius of the excitation laser and v is the velocity of sound. Under our experimental condition, this time constant is nearly 50 ns. Therefore, all of the heat releasing from the process of S_1(enol)–S_0(enol), S_1(enol)–S_1(keto), and S_1(keto)–S_0(enol) (Figure 1) contributes to the fast-rising signal.

We assign the slow rising to the nonradiative decay of the proton back-transfer for the following reasons. First, the only possible slow deactivation process except the proton back-transfer is the decay from the triplet state of the enol or keto forms. The decay rate from the triplet states should be faster than submicrosecond in our air-saturated conditions. Therefore, the decay from the triplet states cannot be the origin of the slow rising. Second, the decay of singlet oxygen created by the quenching of the triplet state is another candidate for the origin of the slow rising. However, we conclude that the contribution of the singlet oxygen decay can be safely neglected, because we could not observe the slow-rising component with the lifetime of 10 μs, which is the reported lifetime of singlet oxygen in methanol[12] (vide infra). Moreover, the rising part does not change even if the solution is deoxygenated by nitrogen bubbling. The quantum yield of the triplet formation of 7-hydroxquinoline is considered to be small. Third, the rising curve is expressed well as single-exponential form (Figure 2) with a lifetime of 3.7 μs. This lifetime agrees with

(2) Crooks, J. E. *Proton Transfer*; Bamford, C. H., Tipper, C. F. H., Eds.; Elsevier Scientific Publishing Co.: New York, 1977.
(3) Mason, S. F.; Philp, P. E. *J. Chem. Soc. A* **1968**, 3051.
(4) Itoh, M.; Adachi, T.; Tokumura, K. *J. Am. Chem. Soc.* **1984**, *106*, 850; *J. Am. Chem. Soc.* **1983**, *105*, 4828.
(5) Tokumura, K.; Itoh, M. *J. Phys. Chem.* **1984**, *88*, 3921.
(6) Thistlethwaite, P. J.; Corkill, P. J. *Chem. Phys. Lett.* **1982**, *85*, 317.
(7) Thistlethwaite, P. J. *Chem. Phys. Lett.* **1983**, *96*, 509.
(8) Carman, R. I.; Kelley, P. I. *Appl. Phys. Lett.* **1968**, *12*, 24.
(9) Terazima, M.; Azumi, T. *Chem. Phys. Lett.* **1987**, *141*, 237.
(10) Terazima, M.; Azumi, T. *Chem. Phys. Lett.* **1988**, *145*, 286.
(11) Bordor, N.; Dewar, M. J. S.; Mayget, A. J. *J. Am. Chem. Soc.* **1970**, *92*, 2929.
(12) Fuke, K.; Ueda, M.; Itoh, M. *J. Am. Chem. Soc.* **1983**, *105*, 1091, and references therein.

that of the keto form in the ground state measured by transient absorption (3.5 μs).[3,4]

By using eq 1 with the experimental result ($U_s/U_t = 0.105$) and the other parameters, $E_{ex} = 29670\ cm^{-1}$, $E_f^e = 26500\ cm^{-1}$, $E_f^k = 18900\ cm^{-1}$, $\phi_f^e = 0.044$,[13] $\phi_f^k = 0.077$,[13] and $\phi_t = 0.85$,[4] ΔH is calculated to be $3400\ cm^{-1}$. It is interesting to note that a quantum mechanically calculated ΔH by Bordor et al. was 2000 cm^{-1},[11] relatively close to the experimental data.

From the spectroscopic data (E_f^e, E_f^k), and the obtained ΔH in the ground state, the stabilization energy of the keto form in the excited (S_1) state is calculated to be $4200\ cm^{-1}$ (Figure 1), much larger than the thermal energy at room temperature. The proton back-transfer rate in the excited state can therefore be negligibly small. This finding supports the kinetic model proposed by Itoh et al.[4]

In summary, we demonstrated that the time-resolved TL method is a very powerful method to measure the enthalpy difference of keto and enol forms in proton-transfer systems.

Registry No. 7-Hydroxyquinoline, 580-20-1.

(13) The quantum yields of fluorescence were determined relative to quinine sulfate in 0.5 M sulfuric acid as a standard solution.

Oxidation of *tert*-Butyl Alcohol to Isobutylene Oxide on a Ag(110) Surface: The Role of Unactivated C–H Bonds in Product Selectivity

Robert L. Brainard† and Robert J. Madix*

Contribution from the Departments of Chemical Engineering and Chemistry, Stanford University, Stanford, California 94305. *Received May 9, 1988*

Abstract: *tert*-Butyl alcohol reacts with oxygen-covered Ag(110) surfaces below 200 K yielding t-$BuO_{(a)}$ and adsorbed water and hydroxyl groups. Temperature-programmed reaction spectroscopy demonstrates that t-$BuO_{(a)}$ reacts at 440 and 510 K by processes that involve rate-limiting C–H bond cleavage yielding isobutylene oxide, isobutylene, *tert*-butyl alcohol, H_2O, and CO_2. The reaction path at 440 K predominates when the initial coverage of $O_{(a)}$ is high; that at 510 K predominates when the coverage of $O_{(a)}$ is low. A third process occurs at 590 K, producing acetone. It is concluded from this work that the unactivated methyl C–H bonds in t-$BuO_{(a)}$ are significantly more stable toward cleavage by this surface than are the activated C–H bonds in $MeO_{(a)}$ or $EtO_{(a)}$. Isotopic labeling experiments with $^{18}O_2$ show that the surface oxygen present before the *tert*-butyl alcohol dose is not incorporated into the isobutylene oxide, acetone, or *tert*-butyl alcohol products. The reactions occurring at 440 and 510 K appear to involve rate-limiting C–H bond breaking reactions yet do not involve transfer of hydrogen atoms to the surface. Instead, direct proton transfer from the methyl group of t-$BuO_{(a)}$ to either $O_{(a)}$ (440 K) or another t-$BuO_{(a)}$ (510 K) appears to occur.

The oxidation of primary and secondary alcohols on Ag(110) and Cu(110) surfaces under ultrahigh vacuum conditions (UHV) is now fairly well understood.[1-5] Generally, the first step involves the reaction of an adsorbed alcohol molecule with surface oxygen to form a surface-bound alkoxide and water (eq 1; R = H, alkyl).

$$2R_2CHOH_{(a)} + O_{(a)} \rightarrow 2R_2CHO_{(a)} + H_2O \quad (1)$$

$$R_2CHO_{(a)} \rightarrow R_2C{=}O + H_{(a)} \quad (2)$$

$$H_{(a)} + R_2CHO_{(a)} \rightarrow R_2CHOH \quad (3)$$

$$2H_{(a)} + O_{(a)} \rightarrow H_2O \quad (4)$$

$$2H_{(a)} \rightarrow H_2 \quad (5)$$

Upon further heating, the surface alkoxide reacts and yields an aldehyde (or ketone) and $H_{(a)}$, presumably by reaction of the hydrogen α to oxygen with the surface (eq 2). Recombination reactions produce the parent alcohol, water, and/or H_2 (eq 3-5). Displacement reactions between surface alkoxides produced as in eq 1 and other alcohols or other proton donors have been useful in establishing a scale of stabilities of the surface alkoxides that agrees with the relative gas-phase acidities of the respective alcohols.[6,7]

The activation energies of reactions occurring according to eq 2 correlate with the bond strength of the C–H bond α to oxygen.[5] In general, these C–H bonds are weaker than "unactivated" C–H bonds by 4–7 kcal/mol due to their proximity to oxygen. An unactivated C–H bond is defined[8] as a C–H bond that is not α to a heteroatom or an unsaturated center. The activated C–H bonds are weaker (have lower bond dissociation energies) because homolytic cleavage of these bonds produces carbon-centered radicals that are stabilized by the adjacent heteroatoms or unsaturated centers.

Scheme I. Reaction of *tert*-Butyl Alcohol (d_0, d_1) on Preoxygenated Ag(110) Surface

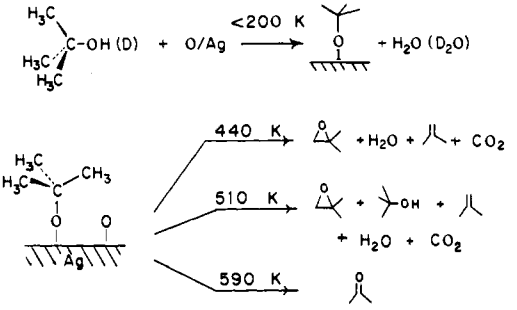

[a] Products of the reactions occurring at 440 and 510 K are listed in order of decreasing yield.

† Current address: Polaroid Corp., 1265 Main Street, W4-2A, Waltham, MA 02254.

(1) Wachs, I. I.; Madix, R. J. *Surf. Sci.* **1978**, *76*, 531-558.
(2) Wachs, I. E.; Madix, R. J. *Appl. Surf. Sci.* **1978**, *1*, 303-328.
(3) Wachs, I. E.; Madix, R. J. *J. Catal.* **1978**, *53*, 208-227.
(4) Bowker, M.; Madix, R. J. *Surf. Sci.* **1980**, *95*, 190-206.
(5) Bowker, M.; Madix, R. J. *Surf. Sci.* **1982**, *116*, 549-572.
(6) Barteau, M. A.; Madix, R. J. *Surf. Sci.* **1982**, *115*, 355-381.
(7) Barteau, M. A.; Madix, R. J. *Surf. Sci.* **1982**, *120*, 262-272.
(8) Janowicz, A. H.; Bergman, R. G. *J. Am. Chem. Soc.* **1983**, *105*, 3929-3939.

0002-7863/89/1511-3826$01.50/0